# Hydraulic stability of cube-armored mound breakwaters in depth-limited breaking wave conditions

Patricia Mares-Nasarre [a,*], Jorge Molines [b], M. Esther Gómez-Martín [b], Josep R. Medina [b]

[a] *Hydraulic Structures and Flood Risk, Faculty of Civil Engineering and Geosciences, Delft University of Technology, the Netherlands*
[b] *Lab. Ports and Coasts, Institute of Transport and Territory, Universitat Politècnica de València, Spain*

## ARTICLE INFO

## ABSTRACT

Armor erosion due to wave attack has been studied intensively since it is considered the main failure mode of mound breakwaters. Cube-armored mound breakwaters in depth-limited breaking wave conditions are common in practice but have received limited attention in the literature. In this study, 2D physical tests were performed on non-overtopped double-layer randomly-placed cube-armored mound breakwater models with armor slope $cot\alpha = 1.5$ and bottom slope $m = 2\%$ in breaking wave conditions. Using the experimental results, a new hydraulic stability formula was derived with a coefficient of determination $R^2 = 0.85$ based on a power relationship between the armor damage and the stability number and the dimensionless water depth. A lower hydraulic stability was found for the front slope of non-overtopped cube-armored structures in breaking wave conditions when compared to formulas given in the literature.

## 1. Introduction

Rubble mound breakwaters built with natural rocks have been used to protect port areas for centuries. Over time, the continuous growth of ports led to breakwaters which had to face more severe wave storms as they were built in deeper waters and outside the naturally protected areas. Since available quarries were not able to provide rocks of the needed size, parallelepiped blocks and cubes made of concrete were included as artificial armor units in the nineteenth century. During the twentieth century, different concrete armor units (Tetrapod, Dolos, etc.) were developed and implemented to optimize the design of the armor layer of mound breakwaters. Nevertheless, the cube is still the most widely used concrete armor unit due to its simplicity and robustness (e. g., Spanish breakwaters described by MOPU, 1988 and MFOM, 2012).

Armor erosion due to wave attack is considered one of the main failure modes when designing mound breakwaters. Consequently, the hydraulic stability of the armor layer has been the focus of numerous studies (e.g., Hudson, 1959 and Van der Meer, 1988a). The majority of these studies were based on physical model tests performed with rock armors in non-breaking wave conditions. However, most mound breakwaters are built in the surf zone where a percentage of the waves which reach the structure have previously broken; thus, the formulas

derived in non-breaking wave conditions are not fully valid (Herrera et al., 2017). The few studies conducted in breaking wave conditions only considered rock-armored breakwaters (e.g., Van Gent et al., 2004; and Herrera et al., 2017) or structures with a relevant overtopping (e.g., Mares-Nasarre et al., 2021a). Therefore, to better design non-overtopped cube-armored mound breakwaters in depth-limited breaking wave conditions, a new method is required to reliably estimate the armor damage to this kind of structure in these specific conditions.

This study focuses on the hydraulic stability of non-overtopped double-layer randomly-placed cube armors in depth-limited breaking wave conditions. 2D physical model tests were conducted in the wave flume of the Laboratory of Ports and Coasts at the Universitat Politècnica de València (LPC-UPV); models were placed on a $m = 2\%$ bottom slope with armor slope $cot\alpha = 1.5$. Based on the results of these physical model tests, a new hydraulic stability formula was derived.

This paper is organized as follows. In Section 2, a brief review of the literature related to the armor damage to mound breakwaters in breaking wave conditions is provided. In Section 3, the experimental set up is described. In Section 4, experimental data are analyzed. In Section 5, a new hydraulic stability formula valid for cube-armored breakwaters in depth-limited breaking wave conditions is derived. In Section 6, the

---

new formula is compared to other formulas given in the literature. Finally, in Section 7, conclusions are drawn.

## 2. Literature review

As mentioned, studies in the literature related to the armor damage to mound breakwaters were performed mainly in non-breaking conditions. Here, a brief review on the hydraulic stability of mound breakwaters is presented, paying special attention to mound breakwaters built in the surf zone.

### 2.1. Armor damage measurement

Armor damage is normally evaluated using both qualitative criteria and quantitative techniques. Qualitative criteria are applied to describe the subjective severity of the damage while quantitative measurements provide an objective value of the damage. In this section, both qualitative criteria and quantitative techniques are summarized.

Four qualitative levels of armor damage were proposed in Losada et al. (1986) and Vidal et al. (1991) for conventional double-layer armors:

1. Initiation of Damage (IDa): some armor units are lost from the upper armor and holes whose size is close to the armor unit are clearly visible;
2. Initiation of Iribarren's Damage (IIDa): units from the bottom armor layer may be extracted, since a large area of the upper armor is eroded;
3. Initiation of Destruction (IDe): at least one element from the bottom armor layer is extracted, so the filter is clearly visible;
4. Destruction (De): elements from the filter layer are removed.

Later, Gómez-Martín (2015) modified these damage levels in order to extend them to conventional mound breakwaters with single-layer armors.

The quantitative measurement of armor damage to mound breakwaters is a complex problem, since it needs to be standardized considering different armor slopes, armor units and number of layers. Three definitions for quantitative armor damage are given in the literature: (1) the relative damage number, $N_{od}$, (2) the percentage of displaced units, $D\%$, and (3) the dimensionless armor damage parameter, $S$. $N_{od}$ and $D\%$ are calculated by counting the displaced units (e.g., USACE, 1975; 1984; Van der Meer, 1999) while S is originally calculated by measuring armor profiles. In this study, an equivalent dimensionless armor damage parameter, $S_e$ is calculated counting the displaced units (see Gómez-Martín and Medina, 2006).

The relative damage number was proposed by Van der Meer (1988b) as $N_{od} = N_e/(d/D_n)$, where $N_e$ is the number of displaced units from a reference band of the armor of width $d$, and $D_n = M/\rho$ is the nominal diameter or equivalent cube size, where $M$ is the mass of the unit, and $\rho$ is the mass density of the unit. Thus, $N_{od}$ represents the number of units extracted from the armor in a band with a width of one $D_n$.

The percentage of displaced units is defined as $D\% = N_d/N_T$, where $N_d$ is the number of extracted or displaced units and $N_T$ is the total number of units within a reference area. This reference area can be the whole armor or an area of the armor between two reference levels (e.g., Van der Kreek, 1969, or USACE, 1984).

The dimensionless armor damage parameter proposed by Broderick (1983) is defined as $S = A_e/D_n^2$, where $A_e$ is the average eroded cross-section area. $A_e$ can be calculated using the visual counting method proposed by Vidal et al. (2006) or using mechanical or laser profilers. These methods assume a constant armor porosity during the erosive process, so the Heterogeneous Packing (HeP) failure mode defined by Gómez-Martín and Medina (2014) is not considered. HeP failure mode refers to the armor damage caused by a reduction in the local packing density of the armor layer near the still water level and an

increase in the local packing density of the armor layer near the toe berm. HeP is especially important in cube armor layers because of their undesired tendency to face-to-face arrangements after the attack of several wave storms. In the previous definition, the packing density refers to the dimensionless concrete consumption for the armor layer, which was pointed out by Medina et al. (2014) as a key parameter in the cube armor stability under non-breaking wave conditions. Thus, neither visual counting nor armor profiling are adequate to analyze damage progression of armors composed of armor units with significant HeP, such as parallelepiped blocks and cubes. Fig. 1 represents the HeP failure mode in a cube armor.

The Virtual Net method was proposed by Gómez-Martín and Medina (2006) in order to consider the armor erosion caused by changes in the armor porosity and, thus, involves both armor unit extraction and the HeP. The Virtual Net method consists of dividing the upper layer of the armor in strips of constant width ($w = aD_n$) and length ($l = bD_n$). The dimensionless damage is calculated independently in each strip ($S_i$) based on the porosity evolution in time and space. In case of an element divided between two strips, it is assigned to the strip where the element presents the highest percentage of its area. In case of several elements divided between two strips, they are distributed so the number of units in each strip is balanced according to the percentage of the areas in each strip. The equivalent dimensionless armor damage parameter ($S_e$) is determined by integrating $S_i$ over the slope, as shown in Eq. (1).

$$S_e = \sum_{i=1}^{I} S_i = \sum_{i=1}^{I} a\left(1 - \frac{1-p_i}{1-p_{i0}}\right) = \sum_{i=1}^{I} a\left(1 - \frac{\varphi_i}{\varphi_{i0}}\right) \tag{1}$$

where $a$ is the number of rows in the strip, $I$ is the number of strips, $p_i = 1-(N_iD_n^2/(wl))$ is the armor porosity of the strip $i$ after the wave attack, being $N_i$ the number of armor units in the strip $i$, $p_{0i}$ is the initial armor porosity of the strip $i$, $\Phi_i = n(1-p_i)$ is the packing density of the strip $i$ after the wave attack, being $n$ the number of armor layers, and $\Phi_{0i}$ is the initial packing density of the strip $i$. Fig. 2 presents an application of the Virtual Net method.

Since the focus of this study is the hydraulic stability of cube-armored structures, the Virtual Net method is applied to account for both armor unit extraction and HeP. Regarding the qualitative analysis of the armor damage, IDa and IDe as defined by Losada et al. (1986) and Vidal et al. (1991) are considered.

### 2.2. Hydraulic stability of mound breakwaters in breaking wave conditions

The most popular independent variable to analyze the hydraulic stability of armor layers is the stability number, $N_s = H/\Delta D_n$, where $H$ is a characteristic wave height, $\Delta = (\rho-\rho_w)/\rho_w$ is the relative submerged mass density of armor units, $\rho$ is the mass density of the armor units, and $\rho_w$ is the mass density of the sea water. The stability number was used in Eq. (2), the generalized stability formula given by Hudson (1959), which was based on small-scale physical tests of non-overtopped mound breakwaters under regular waves in non-breaking wave conditions. In this formula, $K_D$ is the stability coefficient, which depends on the number of armor layers, the armor unit and the section of the breakwater (trunk or head), and $\cot\alpha$ is the armor slope.

$$\frac{H}{\Delta D_n} = (K_D \cot \alpha)^{1/3} \tag{2}$$

USACE (1975 and 1984) recommended modifying the value of $K_D$ in Eq. (2) to account for depth-limited breaking wave conditions. USACE (1975 and 1984) reduced the value of $K_D$ for the same armor layer in breaking compared to non-breaking wave conditions; e.g., $K_D = 7.5$ for a trunk section with a double-layer randomly-placed modified cube armor in non-breaking wave conditions and $K_D = 6.5$ for the same trunk section armor layer in breaking wave conditions. USACE (1984) recommended $K_D = 2.0$ and 6.5 for double-layer rock- and cube-armored breakwaters
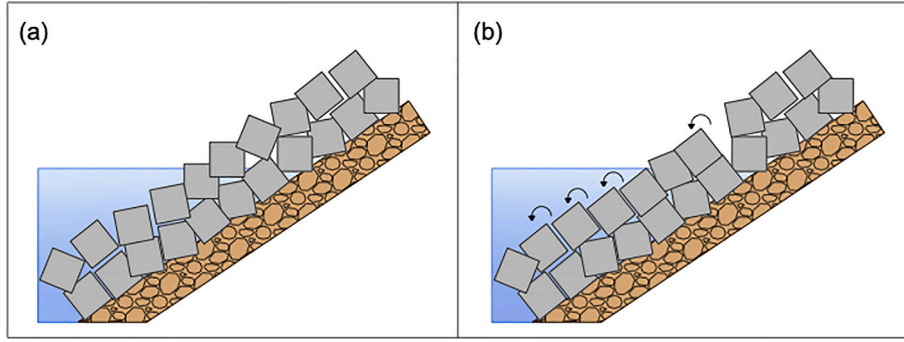
**Fig. 1.** Cube armor failure: (a) initial arrangement, and (b) heterogenous packing (HeP) failure mode.
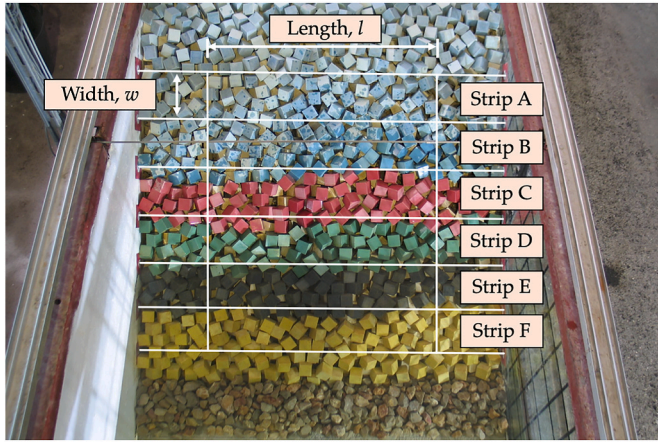


**Fig. 2.** Example of application of the Virtual Net method on the tested double-layer cube-armored model.

in breaking wave conditions for trunk cross-sections, respectively.

Regarding the characteristic wave height in Eq. (2), USACE (1984) recommended using $H=H_{1/10}$ (average of the one-tenth highest waves), while USACE (1975) recommended $H=H_{1/3}$ (average of the one-third highest waves). The change in the criterion between USACE (1975) and USACE (1984) was relevant for non-breaking wave conditions (applying $H_{1/10} = 1.27H_{1/3}$, valid for a storm of 1,000 waves which follows a Rayleigh distribution, leads to approximately double the weight of the required armor element, $1.27^3 = 2.05$). However in breaking wave conditions, this change has less influence; the more relevant the wave breaking, the lower the influence of this change (applying the Composite Weibull distribution by Battjes and Groenendijk (2000) together with a spectral significant wave height $H_{m0} = 4$ $(m_0)^{0.5} = 0.16m$, bottom slope $m = 2\%$ and water depth $h_s = 0.25m$, $H_{1/10} = 1.15H_{1/3}$, which leads to $1.15^3 = 1.52$). USACE (1984) also proposed estimating the design wave height at the breaking point, so the wave height at a certain distance from the toe of the model was considered. It should be noted that structures in depth-limited breaking wave conditions have to face the design waves more frequently than structures built in non-breaking conditions.

Van der Meer (1988a) conducted physical tests mainly in non-breaking wave conditions to analyze the stability of rock armors under wave attack within the ranges $1 \leq H_s/\Delta D_{n50} \leq 4$ and $1.5 \leq cot\alpha \leq 6.0$. Van der Meer (1988a) derived Eq. (3) based on these experimental tests.

$$\begin{cases} \dfrac{H_s}{\Delta D_{n50}} = 6.2S^{1/5}P^{0.18}N_z^{-0.1}\xi_m^{-0.5} \ for \ \xi_m < \xi_{mc} \ (Plunging \ waves) \\[2ex] \dfrac{H_s}{\Delta D_{n50}} = 1.0S^{1/5}P^{-0.13}N_z^{-0.1}\cot\alpha^{0.5}\xi_m P \ for \ \xi_m > \xi_{mc} \ (Surging \ waves) \end{cases}$$ (3)

where $\xi_{mc}=(6.2P^{0.31}tan\alpha^{0.5})^{1/(P+0.5)}$ is the critical breaker parameter, $0.1 \leq P \leq 0.6$ is the permeability coefficient which accounts for the permeability of the structure, $D_{n50}$ is the equivalent cube size of a stone whose mass does not exceed the 50% percentile, $N_z$ is the number of waves and $\xi_m = tan\alpha/(2\pi H_s/[gT_m^2])^{0.5}$ is the surf similarity parameter or Iribarren number calculated using the mean period, $T_m$, and significant wave height, $H_s$.

Van der Meer (1988a) also performed 16 physical tests with a permeable rock-armored slope with $cot\alpha = 2.0$ in breaking wave conditions on a bottom slope $m = 1/30$ and $3.3 \leq h_s/\Delta D_{n50} \leq 6.5$, where $h_s$ is the water depth at the toe of the structure. In order to account for wave breaking, Van der Meer (1988a) recommended replacing $H_s$ in Eq. (3) with $H_{2\%}/1.4$, where $H_{2\%}$ is wave height exceeded by 2% of the waves. Note that $H_{2\%}/H_s \approx 1.4$ for a Rayleigh distribution.

Van Gent et al. (2004) conducted physical tests in both breaking and non-breaking wave conditions using rock slopes with permeable and impermeable cores. Two bottom slopes, $m = 1/30$ and $1/100$, two armor slopes, $cot\alpha = 2.0$ and $4.0$, and two nominal diameters, $D_{n50} = 2.2$ and $3.5$ cm, were considered. Van Gent et al. (2004) combined their results with those reported by Smith et al. (2003) and developed Eq. (4), which is valid within the experimental ranges $0.5 \leq H_s/(\Delta D_{n50}) \leq 4.5$ and $1.5 \leq h_s/(\Delta D_{n50}) \leq 11$.

$$\begin{cases} \dfrac{H_{2\%}}{\Delta D_{n50}} = 8.4S^{1/5}P^{0.18}N_z^{-0.1}\xi_{s-1}^{-0.5} \ for \ \xi_{s-1} < \xi_{mc} \ (Plunging \ waves) \\[2ex] \dfrac{H_{2\%}}{\Delta D_{n50}} = 1.3S^{1/5}P^{-0.13}N_z^{-0.1}\cot\alpha^{0.5}\xi_{s-1}P \ for \ \xi_{s-1} > \xi_{mc} \ (Surging \ waves) \end{cases}$$ (4)

where $\xi_{s-1} = tan\alpha/(2\pi H_s/[gT_{m-1,0}^2])^{0.5}$ is the surf similarity parameter obtained with the spectral period $T_{m-1,0} = m_{-1}/m_0$, in which $m_i$ is the i-th spectral moment.

Van Gent et al. (2004) also proposed Eq. (5) to include the influence of the relative size of the rocks in the core ($D_{n50core}$) compared to the rocks in the armor ($D_{n50}$). Note that the wave period is not considered here.

$$\dfrac{H_s}{\Delta D_{n50}} = 1.75\left(1 + \dfrac{D_{n50core}}{D_{n50}}\right)\left(\dfrac{S}{\sqrt{N_z}}\right)^{1/5}\cot\alpha^{0.5}$$ (5)

Herrera et al. (2017) conducted physical tests with rock armored mound breakwaters with $cot\alpha = 1.5$ in depth-limited breaking wave conditions; these tests were carried out on a bottom slope $m = 2\%$ and experimental ranges $1.0 \leq H_{m0}/(\Delta D_{n50}) \leq 2.5$ and $3.8 \leq h_s/(\Delta D_{n50}) \leq 7.5$, where $h_s$ is the water depth at the toe of the structure. Herrera et al. (2017) indicated that the optimum point (minimum error in subsequent estimations) to measure wave characteristics is relevant in breaking wave conditions and recommended using $H_{m0}$ at a distance of 3 times $h_s$ from the toe of the structure as design wave height. Herrera et al. (2017) also proposed Eq. (6) as the damage function; water depth at the toe ($h_s$) and wave steepness ($s_m = H_{m0}/L_m$, where $L_m$ is the mean wave length close to the model) were discarded as significant variables to estimate

armor damage.

$$S_e = 0.066 \left( \frac{H_{m0}}{\Delta D_{n50}} \right)^6 \qquad (6)$$

Gómez-Martín et al. (2018) performed physical tests with regular waves on double-layer and single-layer Cubipod®-armored breakwaters in depth-limited breaking wave conditions; non-overtopped structures with $cot\alpha = 1.5$ on a horizontal foreshore ($m = 0\%$) were analyzed. Gómez-Martín et al. (2018) proposed new equations to design mound breakwaters for any deep-water wave conditions regardless of the wave height at the toe of the structure; the water depth at a distance of three times the wave depth from the toe, $h = h_s(1 + 3m)$, was used as the design parameter (see Eq. (7)). This approximation is reasonable for gentle bottom slopes ($m \leq 2\%$).

$$D_n > \left( \frac{h}{7\Delta} \right) for\ double-layer\ Cubipod^{®}\ armors \qquad (7a)$$

$$D_n > \left( \frac{h}{6.2\Delta} \right) for\ single-layer\ Cubipod^{®}\ armors \qquad (7b)$$

Etemad-Shahidi et al. (2020) combined physical test results given by Thompson and Shuttler (1975), Van der Meer (1988a), Van Gent et al. (2004), and Vidal et al. (2006) for non-overtopped rubble mound breakwaters in breaking and non-breaking wave conditions. New formulas were derived, these being valid within the ranges $1.0 \leq H_s/(\Delta D_{n50}) \leq 4.3$ and $1.35 \leq h_s/H_s \leq 19.68$ for both breaking and non-breaking wave conditions.

$$\begin{cases} \dfrac{H_s}{\Delta D_{n50}} = 4.5 C_p N_z^{-0.1} S^{1/6} \xi_{s-1}^{-7/12} (1-3m)\ for\ \xi_{s-1} < 1.8\,(plunging\ waves) \\[2mm] \dfrac{H_s}{\Delta D_{n50}} = 3.9 C_p N_z^{-0.1} S^{1/6} \xi_{s-1}^{-1/3} (1-3m)\ for\ \xi_{s-1} \geq 1.8\,(surging\ waves) \end{cases} \qquad (8)$$

where $C_p = (1 + [D_{n50core}/D_{n50}]^{3/10})^{3/5}$ is the coefficient of permeability. Note the 6-power relationship between the stability number and dimensionless armor damage in Eqs. (6) and (8).

Recently, Mares-Nasarre et al. (2021a) re-analyzed the tests reported by Argente (2019) with overtopped mound breakwaters in depth-limited breaking wave conditions. These tests considered mound breakwaters with $cot\alpha = 1.5$ and three armor layers: double-layer randomly-placed rock, double-layer randomly-placed cube, and single-layer randomly-placed Cubipod® armors. New formulas similar to Eq. (6) were fitted for the front slope, crest and rear side; the front slope of overtopped structures was more stable than that of non-overtopped structures. Eq. (9) presents the formula derived for the front slope of the cube-armored model.

$$S_e = 0.05 \left( \frac{H_{m0}}{\Delta D_n} \right)^3 \qquad (9)$$

In this section, formulas in the literature to describe the hydraulic stability of mound breakwaters in breaking wave conditions have been summarized; no specific study focuses on the armor damage to non-overtopped cube-armored breakwaters in breaking wave conditions. The formulas given in the literature for cube-armored structures in breaking wave conditions were conducted on overtopped structures. Thus, further research is needed to better design non-overtopped cube-armored mound breakwaters in depth-limited breaking wave conditions.

## 3. Experimental methodology

Two-dimensional physical model tests were conducted in the LPC-UPV wave flume (30 m × 1.2 m × 1.2 m). The wave flume had a 6.25 m-long $m = 4\%$ ramp followed by a 9.00 m-long $m = 2\%$ ramp, as

shown in Fig. 3.

Surface elevation was measured using 13 capacitive wave gauges placed along the wave flume as indicated in Fig. 3. In the wave generation zone, four wave gauges (S1 to S4) were located in order to separate incident and reflected waves. Eight wave gauges (S5 to S12) were placed along the flume and close to the model, and an additional wave gauge (S13) was installed behind the model to monitor the water level at the end of the flume. Since the model was built in the surf zone, where depth-limited wave breaking occurs, methods given in the literature are not reliable to separate incident and reflected waves.

Double-layer randomly-placed cube-armored breakwater models were tested with $D_n = 3.97$ cm, armor slope $cot\alpha = 1.5$, rock toe berms ($D_{n50} = 2.47$ cm), a filter layer with $D_{n50} = 1.78$ cm and a core with $D_{n50} = 0.68$ cm. The initial packing density of the cube armors was $\Phi_0 = 2(1-p) = 1.18$, where $p$ is the armor porosity (Medina et al., 2014). The cross-section is depicted in Fig. 4 while Table 1 describes the characteristics of the materials used during the tests.

Random runs of 1,000 irregular waves were generated using a piston-type wave maker following a JONSWAP spectrum ($\gamma = 3.3$). The active wave absorption system (AWACS) was used to prevent multi-reflections in the wave flume. Low-frequency oscillations and changes in the still water level (e.g.: set-up) were prevented by allowing the water to recirculate through a double floor.

Three water depths at the toe of the structure were considered, $h_s$(m) $= 0.20, 0.30$ and $0.40$. The test series for each water depth were conducted with a constant wave steepness ($s_{0p} = H_{m0}/L_{0p} = 2\pi H_{m0}/(gT_p^2)$, where $L_{0p}$ is the deep-water wave length calculated using the peak period, $T_p$). For $h_s$(m) $= 0.20$, $s_{0p} = 0.02$ and $0.05$ were tested, and for $h_s$(m) $= 0.30$, $s_{0p} = 0.02, 0.03$ and $0.05$ were considered. Only $s_{0p} = 0.05$ was tested for $h_s$(m) $= 0.40$, in order to prevent overtopping. In each test series, $H_{m0}$ at the wave generation zone was increased in steps of 1 cm from no damage to initiation of destruction of the cube armor or wave breaking observed at the wave generation zone. Experimental ranges of the main variables in the tests are shown in Table 2; incident wave characteristics ($H_{m0}$ and $T_p$) are given at a distance of $3h_s$ from the toe of the model following recommendations by Herrera et al. (2017).

## 4. Data analysis

The data analysis is described in this section including the methodology to determine the incident wave characteristics in the model zone as well as the equivalent dimensionless armor damage ($S_e$) after each test.

### 4.1. Wave analysis

As explained in Section 3, wave gauges in the wave generation zone (S1 to S4) were used to separate incident and reflected waves using the LASA-V method (Figueres and Medina, 2005). Although this method can be applied to non-stationary and non-linear irregular waves, it is not reliable for breaking waves, similar to other methods given in the literature. Thus, the SwanOne model (Verhagen et al., 2008) was used here to estimate incident wave characteristics close to the model where depth-induced wave breaking occurs. The SwanOne model fits a JONSWAP spectrum ($\gamma = 3.3$) to the given incident wave conditions in the wave generation zone. This spectrum is propagated along an input bathymetry, and the Composite Weibull distribution proposed by Battjes and Groenendijk (2000) is assumed to describe the wave height distribution in shallow foreshores. A reference scale 1/30 was used in the propagation, since the SwanOne model considers frequencies within a range typical for prototype scale (0.03–0.8 Hz).

Following recommendations by Herrera et al. (2017), the results provided by the SwanOne model were validated using tests without a structure. Those tests were performed with an efficient passive wave absorption system at the end of the flume ($K_r = H_{m0,r}/H_{m0,i} < 0.25$, where $H_{m0,r}$ is the reflected $H_{m0}$, and $H_{m0,i}$ is the incident $H_{m0}$). In order to
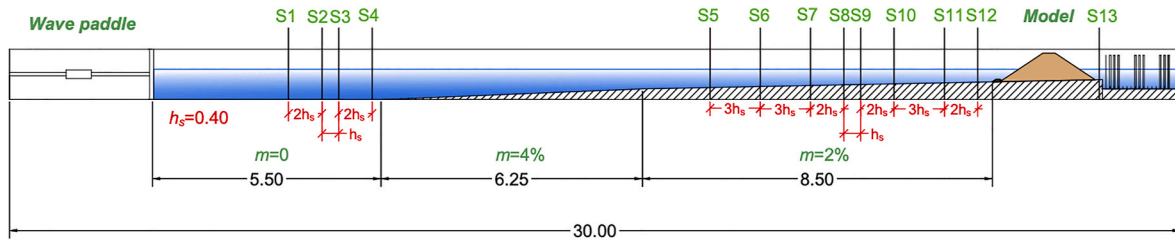
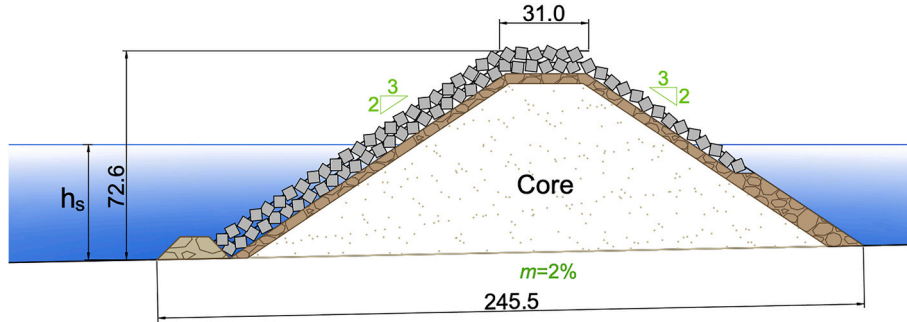**Fig. 3.** Longitudinal cross-section of the LPC-UPV wave flume.



**Fig. 4.** Cross-section of the tested cube-armored breakwater model. Dimensions in cm.

**Table 1**
Characteristics of the materials used during the physical tests.

| Material | $M$ or $M_{50}$ (g) | $\rho$ or $\rho_r$ (g/cm³) | $D_n$ or $D_{n50}$ (cm) |
|---|---|---|---|
| Cube | 141.51 | 2.27 | 3.97 |
| Rock (filter) | 15.40 | 2.73 | 1.78 |
| Rock (core) | 0.86 | 2.72 | 0.68 |
| Toe berm | 40.0 | 2.64 | 2.47 |

**Table 2**
Incident wave characteristics in the physical tests.

| #tests | $h_s$ [m] | $s_{0p}$ [-] | $H_{m0}$ [m] | $T_p$ [s] |
|---|---|---|---|---|
| 14 | 0.20 | 0.02 | 0.08–0.13 | 1.6–2.5 |
| 16 | 0.20 | 0.05 | 0.05–0.13 | 1.0–1.6 |
| 14 | 0.30 | 0.02 | 0.07–0.19 | 1.6–2.8 |
| 17 | 0.30 | 0.03 | 0.06–0.19 | 1.3–2.6 |
| 16 | 0.30 | 0.05 | 0.05–0.18 | 1.0–1.8 |
| 16 | 0.40 | 0.05 | 0.05–0.19 | 1.0–1.6 |

validate the results of the SwanOne model, the incident wave conditions were compared to the measurements during the tests without a structure (total waves) at both the wave generation zone and the model zone. Thus, the capability of the SwanOne model to fit the JONSWAP spectrum with the given incident wave conditions was also assessed. It should be noted that the average wave characteristics measured during the tests without structure in S1 to S4 and S9 to S12 were considered for comparison in the wave generation and model zone, respectively.

In order to evaluate the performance of SwanOne model, two statistical criteria were applied: (1) the correlation coefficient ($r$), and (2) the coefficient of determination ($R^2$). $0 \leq r \leq 1$ evaluates the correlation and $0 \leq R^2 \leq 1$ estimates the proportion of variance explained by the model. Thus, the higher the $r$ and the higher the $R^2$, the better.

$$r = \frac{\sum_{i=1}^{N_o}(o_i - \overline{o})(e_i - \overline{e})}{\sqrt{\sum_{i=1}^{N_o}(o_i - \overline{o})^2 \sum_{i=1}^{N_o}(e_i - \overline{e})^2}} \tag{10}$$

$$R^2 = 1 - \frac{\frac{1}{N_o}\sum_{i=1}^{N_o}(o_i - e_i)^2}{\frac{1}{N_o}\sum_{i=1}^{N_o}(o_i - \overline{o})^2} \tag{11}$$

where $N_o$ is the number of observations, $o_i$ and $e_i$ are the observations and estimations, and $\overline{o}$ is the average of the observations.

First, $H_{m0}$ given by the SwanOne model is compared to the measured $H_{m0}$ during tests without a structure, as shown in Fig. 5. A good performance of the SwanOne model can be observed both in the wave generation zone ($R^2 = 1.00$) and the model zone ($R^2 = 0.94$).

Three characteristic wave periods were estimated: (1) the peak period, $T_p$, (2) the mean spectral period, $T_{01} = m_0/m_1$, where $m_i$ is the i-th spectral moment, and (3) the spectral period, $T_{m-1,0} = m_{-1}/m_0$. The best estimations by SwanOne were provided for $T_p$ ($R^2 > 0.94$), as shown in Fig. 6.

Figs. 7 and 8 compare the measured $T_{01}$ and $T_{m-1,0}$ with the estimations by the SwanOne model. In both cases, results were poor in the model zone, as previously reported by Mares-Nasarre et al. (2020b, 2021b); measured $T_{01}$ and $T_{m-1,0}$ were between 5% to 10% and 10%–40%, respectively, higher than estimations given by SwanOne. Measured low-frequency wave components were more energetic than those predicted by SwanOne.

In the present study, wave characteristics provided by the SwanOne model are used, since the design wave conditions at the construction site need to be estimated during the design phase. In the following sections, $T_p$ is used as the representative wave period since it was accurately estimated by the SwanOne model. In this study, a one-peak wave spectrum (JONSWAP) is considered, so the different wave periods are correlated, making this decision non-critical. However, it would be necessary to assess the most appropriate wave period if wave conditions with multiple-peak spectrums were analyzed.

### 4.2. Armor damage analysis

As mentioned in Section 2.1, the Virtual Net method proposed by Gómez-Martín and Medina (2006) is applied to quantify armor damage due to the HeP failure mode. To this end, a camera was installed perpendicular to the slope, and pictures were taken before starting the tests and after each test, so damage evolution could be studied over time.
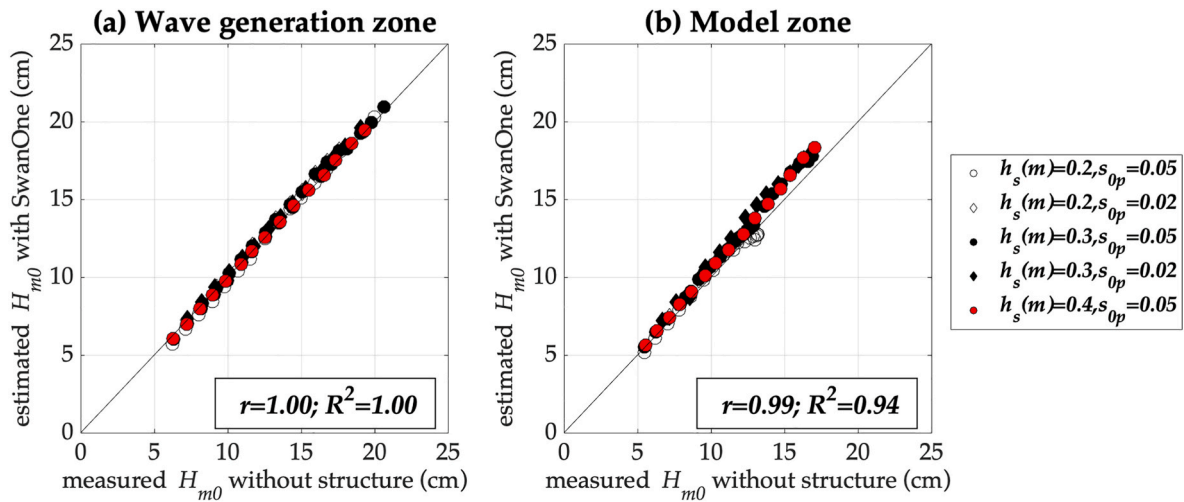
**Fig. 5.** The measured spectral wave height in tests without a structure (total waves) compared to the incident spectral wave height estimated with the SwanOne model: (a) in the wave generation zone, and (b) in the model zone.
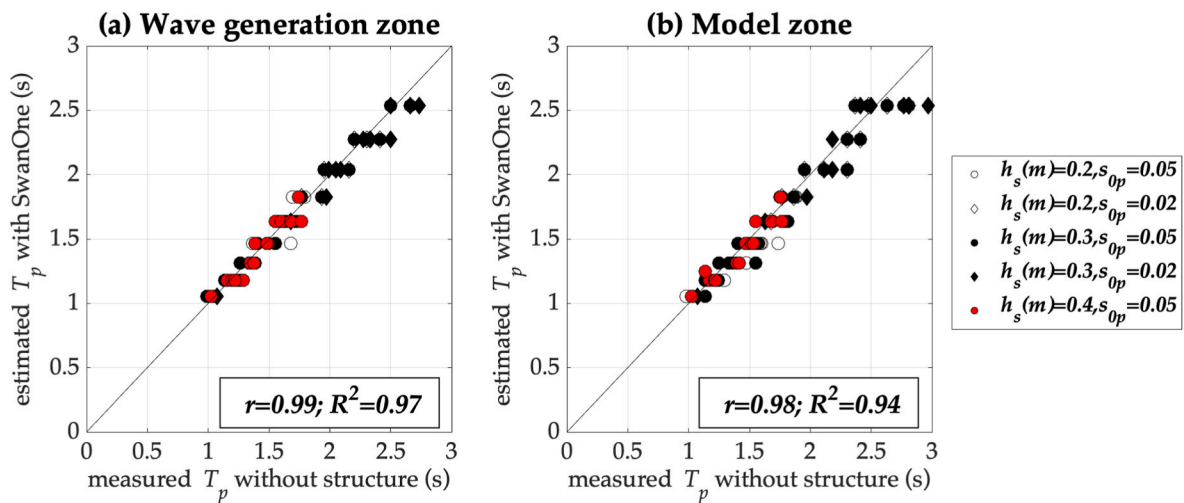


**Fig. 6.** The measured peak period $T_p$ in tests without a structure compared to the peak period estimated with the SwanOne model: (a) wave generation zone, and (b) model zone.
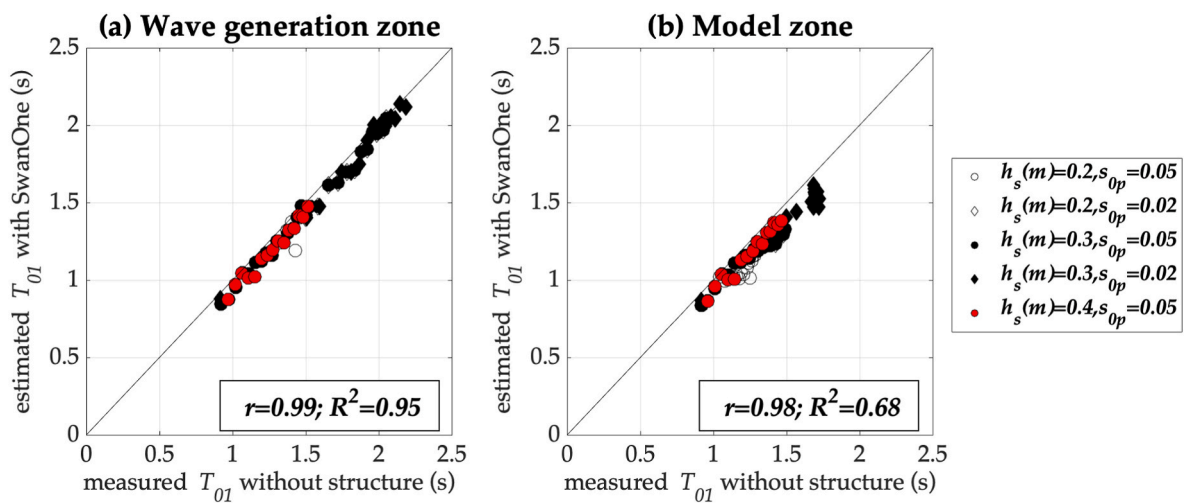


**Fig. 7.** The measured mean spectral period $T_{01}$ in tests without a structure compared to the mean spectral period estimated with the SwanOne model: (a) wave generation zone, and (b) model zone.
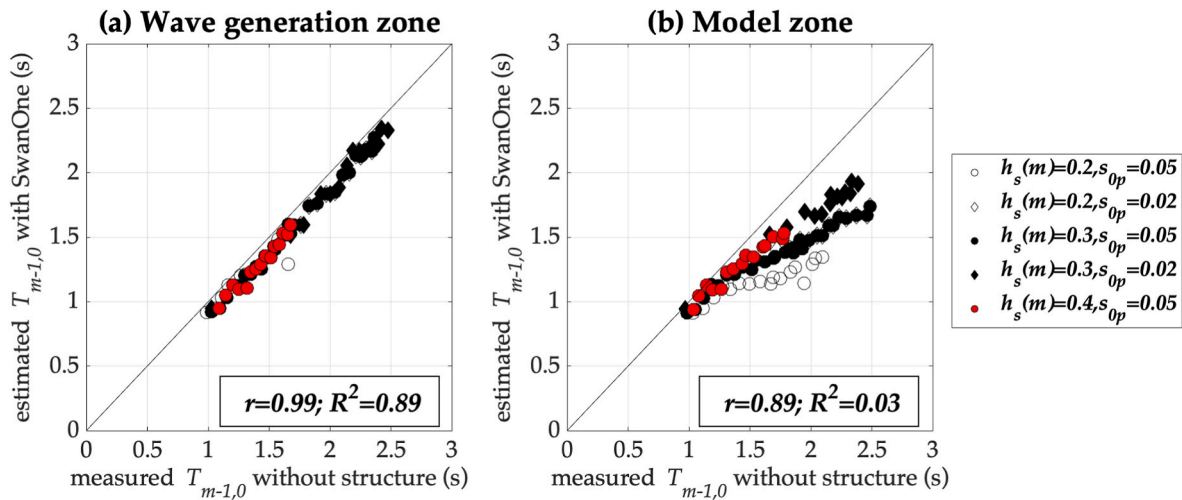
**Fig. 8.** The measured spectral period $T_{m-1,0}$ in tests without a structure compared to the spectral period $T_{m-1,0}$ estimated with the SwanOne model: (a) wave generation zone, and (b) model zone.

The slope was divided in 6 strips of $4D_n$ and only the central part of the slope was considered in order to avoid interference caused by the boundaries of the flume. As shown in Fig. 2, the two upper and two lower rows of the front slope were also discarded from the analysis to prevent interferences with the crest and the toe berm. Following Eq. (1), $S_i$ was obtained for each strip after each test and it was integrated to determine $S_e$. Fig. 2 shows an example of the application of the Virtual Net method. A summary of the experimental data reported in this study is provided in Appendix A.

The qualitative armor damage assessment was conducted considering IDa and IDe levels following the recommendations given by Losada et al. (1986) and Vidal et al. (1991) recommendations (see Section 2.1). IDa and IDe levels were determined at $S_e(IDa) \approx 0.6$ and $S_e(IDe) \approx 5$, which approximately correspond to $N_s(IDa) \approx 2.3$ and $N_s(IDe) \approx 3.5$. It should be noted that IDe was not observed during tests with $h_s(m) = 0.20$ due to wave breaking before wave trains reached the structure. Fig. 9 presents an overview of the experimental data, as well as the IDa and IDe levels in this study.
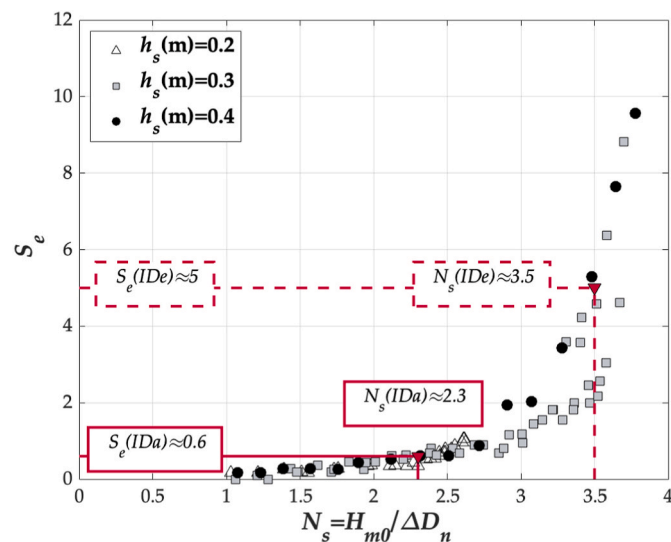


**Fig. 9.** Experimental armor damage data and Initiation of Damage (IDa) and Initiation of Destruction (IDe) levels.

## 5. A new hydraulic stability formula

In this section, the observed armor damage is described, and a new hydraulic stability formula valid for cube armors in depth-limited breaking wave conditions is derived.

### 5.1. Explanatory variables

Four dimensionless variables were first considered as possible explanatory variables to estimate the armor damage to cube-armored mound breakwaters in depth-limited breaking wave conditions:

- $N_s = H/(\Delta D_n)$ is the stability number, a widely used explanatory variable to estimate armor damage (e.g., Eqs. (2)–(6)).
- $h_s/(\Delta D_n)$ is the dimensionless water depth (e.g., Eq. (7)). This variable represents the degree to which the mound breakwater is under depth-limited breaking wave conditions. When the structure is located in shallow waters, $\Delta D_n$ is close to $h_s$, while in deep waters, $\Delta D_n$ is much smaller than $h_s$.
- $H/L_p$, is the wave steepness calculated using $T_p$. This variable determines the type of wave breaking on the slope and it can be found in formulas in the literature to describe armor damage (e.g., Eqs. (3), (4) and (8)).
- $h_s/L_p$, is the dimensionless water depth using $h_s$ at the toe of the structure and the wave length calculated as $L_p = gT_p^2/(2\pi)$, where $g$ is the gravity acceleration. This variable was recommended by Díaz-Carrasco et al. (2020) together with $H/L_p$ to describe wave characteristics and wave breaking in permeable and impermeable slopes. The aforementioned authors also stated that this variable influences the amount of wave energy which is dissipated, transmitted and reflected by mound breakwaters.

Different characteristic wave heights ($H$) are recommended for the formulas given in the literature. For instance, Van Gent et al. (2004) considered $H_{2\%}$ at the toe of the structure whereas Herrera et al. (2017) proposed using $H_{m0}$ measured at a distance of $3h_s$ from the toe of the structure. In this study, $H_{m0}$, $H_{2\%}$ and the average wave height of the one-tenth highest waves, $H_{1/10}$, are considered for further analysis. In depth-limited breaking wave conditions, Herrera et al. (2017) pointed out that it is crucial to select the appropriate point to estimate wave characteristics. Thus, wave characteristics at different locations were considered in this study; wave characteristics at the toe, at a distance of $h_s$ from the toe of the model, $2h_s$, $3h_s$, and so on until $6h_s$ from the toe of the structure were measured.

### 5.2. General outline

Based on the literature review, Eq. (12) was assumed as a potential model for the new hydraulic stability formula,

$$S_e = k_1 \left(\frac{H}{\Delta D_n}\right)^{k_2} \left(\frac{h_s}{\Delta D_n}\right)^{k_3} \left(\frac{H}{L_p}\right)^{k_4} \left(\frac{h_s}{L_p}\right)^{k_5} \tag{12}$$

where $k_1$, $k_2$, $k_3$, $k_4$ and $k_5$ are parameters and $H=H_{m0}$, $H=H_{2\%}$ or $H=H_{1/10}$.

Calculating logarithms on both sides of the equation, Eq. (12) is linearized, and a forward stepwise linear regression is applied to determine which variables are significant to describe cube armor damage. First, four models considering only one of the explanatory variables are calibrated and their significance is evaluated using t-student test (5% significance level). Second, three models are created considering the most significant variable from the previous step and each one of the remaining explanatory variables. This step-by-step methodology is used to create a model with the most significant variables; the methodology ends when all the significant explanatory variables are included or the remaining explanatory variables are not significant. Tests with $S_e < 0.2$ were removed from the analysis.

The process described above was repeated considering $H=H_{m0}$, $H=H_{2\%}$ and $H=H_{1/10}$, measured at distances of $x$ times $h_s$ from the toe, where $x = 0$ to 6 with $\Delta x = 1$. Therefore, 21 (3 characteristic wave heights × 7 measurement locations) models were analyzed; the goodness-of-fit of these 21 models were assessed using $R^2$. The best results were obtained using $H=H_{m0}$, as in Herrera et al. (2017). Regarding the optimum point to estimate wave characteristics, similar results were observed independently of the $x$. Thus, $H_{m0}$ measured at a distance of $3h_s$ from the toe of the structure was used in this study, following recommendations by Herrera et al. (2017) and Mares-Nasarre et al. (2020a).

The most significant explanatory variable was always the stability number, $N_s = H/(\Delta D_n)$. In 14 of the 21 cases, $h_s/(\Delta D_n)$ was a significant secondary explanatory variable. $H/L_p$ and $h_s/L_p$ were not found to be significant in any case (5% significance level).

### 5.3. A new hydraulic stability formula for cube armors

After analyzing the results described in the previous section, Eq. (12) was proposed to describe cube-armor damage in depth-limited breaking wave conditions with $k_4 = k_5 = 0$ and $H=H_{m0}$ (measured at a distance of $3h_s$ from the toe of the structure).

In order to fit $k_1$ to $k_3$ as well as to characterize their variability, the bootstrapping technique was applied following Mares-Nasarre et al. (2019 and 2021b). The bootstrap resample technique consists of selecting $N$ data randomly from a dataset with $N$ data. Hence, each datum presents a probability of $1/N$ to be selected each time; some data may not appear while others may appear more than once in each resample. Here, 1,000 resamples were performed and Eq. (12) was fitted for each resample, so 1,000 values were obtained for $k_1$, $k_2$ and $k_3$ ($k_4 = k_5 = 0$). The variability of the empirical coefficients was considered to determine the number of significant figures in the final coefficients.

$$S_e = 0.00015 \left(\frac{H_{m0}}{\Delta D_n}\right)^6 \left(\frac{h_s}{\Delta D_n}\right)^{1.5} \tag{13}$$

where $H_{m0} = 4m_0^{0.5}$ is the spectral significant wave height estimated at a distance of $x = 3h_s$ from the toe of the structure, $\Delta = (\rho-\rho_w)/\rho_w$ is the relative submerged mass density of armor units, $\rho$ is the mass density of the armor units, $\rho_w$ is the mass density of the sea water, $D_n$ is the nominal diameter of the armor unit and $h_s$ is the water depth at the toe of the structure.

The best fit was found for $k_1 = 1.5 \cdot 10^{-4}$, $k_2 = 6$ and $k_3 = 1.5$ with $R^2 = 0.85$. Note that the 6-power relationship was also found in Eqs. (6) and (8). Eq. (13) is valid within the ranges $1.4 \le H_{m0}/\Delta D_n \le 3.8$ and $4.0 \le h_s/$

$\Delta D_n \le 8.0$.

Fig. 10a shows the measured and estimated equivalent dimensionless armor damage $S_e$ as function of $N_s$ for $h_s$(m) = 0.3 and 0.4. Fig. 10b compares the measured equivalent dimensionless armor damage $S_e$ with the estimated $S_e$ using Eq. (13); the 90% confidence interval is also depicted.

Since the Mean Squared Error was not constant for increasing values of $S_e$, the methodology used by Molines and Medina (2016) was applied here to estimate the confidence intervals. After analyzing the data, a Gaussian error distribution was assumed with 0 mean and a variance estimated by

$$\sigma^2(\varepsilon) = 0.4 S_e \tag{14}$$

Thus, the 90% confidence interval is given by

$$S_e \big|_{5\%}^{95\%} = S_e \pm 1.64\sqrt{0.4 S_e} = S_e \pm 1.04\sqrt{S_e} \tag{15}$$

## 6. Comparison with existing formulas given in the literature

In the previous sections, data related to armor damage to non-overtopped randomly-placed cube-armors in depth-limited breaking wave conditions were analyzed and Eq. (13) was found. Here, the new formula proposed in this study is compared to those given in the literature for depth-limited breaking wave conditions. Eqs. (5), (6) and (9) given by Van Gent et al. (2004), Herrera et al. (2017) and Mares-Nasarre et al. (2021a), respectively, are compared to Eq. (13). It should be noted that Eqs. (5) and (6) by Van Gent et al. (2004) and Herrera et al. (2017) were developed for rock armors in different ranges of applicability, while Eq. (9) by Mares-Nasarre et al. (2021a) considered only overtopped structures. If the conditions of this study are applied, Eq. (5) by Van Gent et al. (2004) can be rewritten as

$$\frac{H_s}{\Delta D_{n50}} = 1.75 \left(1 + \frac{0.68}{3.97}\right) \left(\frac{S}{\sqrt{1000}}\right)^{0.2} 1.5^{0.5} = 1.26 S^{0.2} \rightarrow S = 0.317 N_s^5 \tag{16}$$

Fig. 11 compares Eq. (13) with Eq. (16) derived from Eq. (5) proposed by Van Gent et al. (2004), Eq. (6) by Herrera et al. (2017) and Eq. (9) by Mares-Nasarre et al. (2021a). Note that the HeP is not dominant in rock armors, so $S \approx S_e$ (see Herrera et al., 2017).

In breaking wave conditions and trunk cross-sections, USACE (1984) recommended $K_D = 6.5$ and 2.0 for modified cube- and double-layer rock-armored breakwaters, respectively; thus, stability numbers for cube armors should be around 50% higher ($1.5 \approx (6.5/2.0)^{1/3}$) than rock armors. Fig. 11 shows a higher hydraulic stability for non-overtopped cube-armors compared to rock-armors in depth-limited breaking wave conditions; the observed stability numbers for cubes are slightly higher than 50% above those corresponding to the rock armors.

Observed armor damage is higher for non-overtopped compared to overtopped cube-armored breakwaters; the front slope of overtopped structures is more stable than that of non-overtopped structures, as reported by Mares-Nasarre et al. (2021a). However, damage starts earlier in overtopped structures. If the same wave height is considered attacking an overtopped and a non-overtopped structure, a higher proportion of the front armor is affected by the incident wave trains in the overtopped breakwater. Thus, this may be the reason why damage is higher in overtopped structures when considering low stability numbers.

Finally, results given with Eq. (13) are compared to those obtained following recommendations by USACE (1984). USACE (1984) recommended Eq. (2) by Hudson (1959), where $H=H_{1/10}$ and $K_D = 6.5$ for modified cube-armored trunk sections. Assuming $H_{m0} = 0.16$m, bottom slope $m = 2\%$ and water depth $h_s = 0.25$m and using the Composite Weibull distribution by Battjes and Groenendijk (2000), $H_{1/10} = 0.18$m. Therefore, considering $cot\alpha = 1.5$, $D_n = 6.8$ cm is required according to USACE (1984). If Eq. (13) is considered instead, $D_n = 4.6$ cm is obtained for IDa level. Thus, it can be concluded that recommendations in USACE (1984) are on the safety side.
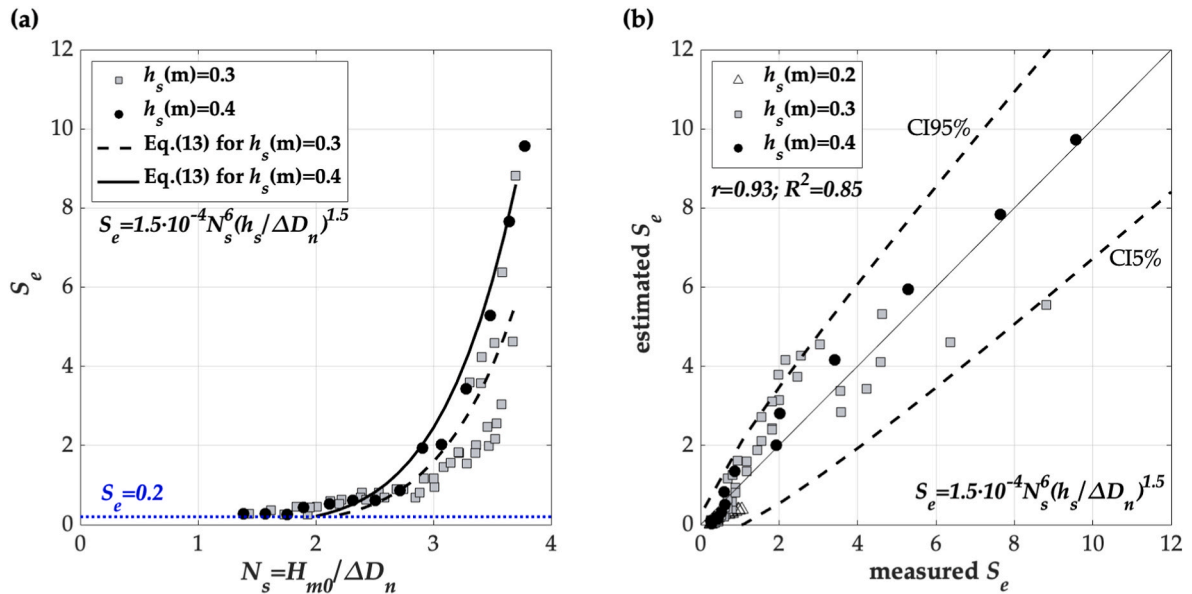
**Fig. 10.** Performance of Eq. (13). Comparison of (a) estimated versus measured $S_e$ as function of $N_s$, and (b) estimated versus measured dimensionless armor damage, $S_e$.
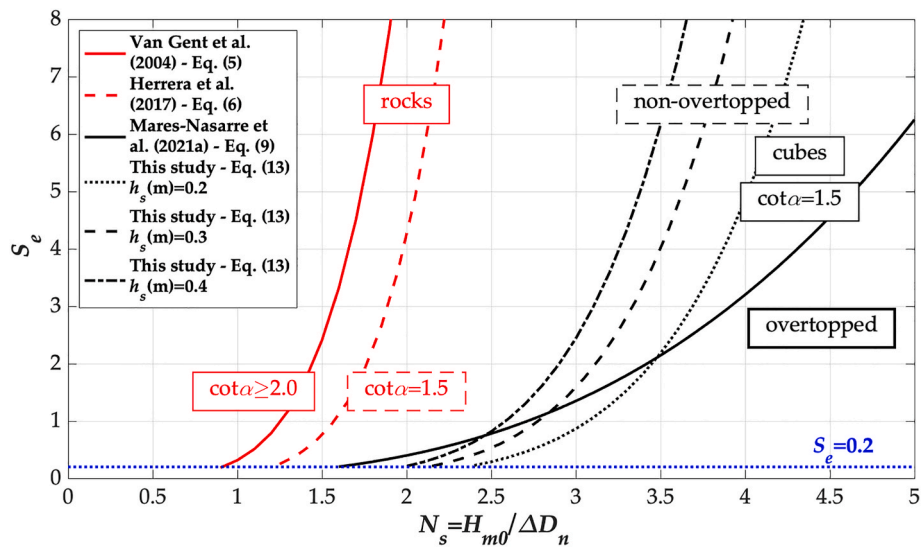


**Fig. 11.** Comparison between Eq. (13) and Eqs. (5), (6) and (9).

## 7. Conclusions

Two-dimensional physical tests were performed in this research to better describe the armor damage to non-overtopped double-layer randomly-placed cube-armored breakwaters in depth-limited breaking wave conditions with $cot\alpha = 1.5$ and bottom slope $m = 2\%$. Based on the new experimental database, quantitative armor damage was analyzed and qualitative IDa and IDe levels were considered.

Four potential explanatory variables were selected from the literature to describe the hydraulic stability of cube-armors in depth-limited breaking wave conditions: (1) the stability number, $N_s = H/(\Delta D_n)$, (2) the dimensionless water depth with the nominal diameter, $h_s/(\Delta D_n)$, (3) the wave steepness, $H/L_p$, and (4) the dimensionless water depth with the wave length, $h_s/L_p$. Only $N_s = H/(\Delta D_n)$ and $h_s/(\Delta D_n)$ were significant variables, being principal and secondary explanatory variables, respectively. A new hydraulic stability formula, Eq. (13), based on a power relationship between the armor damage and the two significant explanatory variables was found with the coefficient of

determination $R^2 = 0.85$.

The new hydraulic stability formula was compared to those given in the literature for mound breakwaters in depth-limited breaking wave conditions. The tested cube-armored breakwater models were found to have a much higher hydraulic stability than the double-layer rock armors in depth-limited breaking wave conditions described in the literature. On the other hand, the non-overtopped cube-armored models tested in this study showed less hydraulic stability than the frontal slope of overtopped cube armors described in the literature. Since part of the wave energy is dissipated through the armored crest and rear side in overtopped structures, the frontal slope of overtopped armors showed less armor damage for high stability numbers.

Eq. (13) is reliable and can be used within the prescribed ranges of application to design non-overtopped cube-armored breakwaters in depth-limited breaking wave conditions. Previous formulas given in the literature are not adequate to design this type of structure in these conditions. Thus, further research is required to better describe armor damage of mound breakwaters in depth-limited breaking wave

conditions, considering different armor elements and different armor slopes.

## CRediT authorship contribution statement

**Patricia Mares-Nasarre:** Conceptualization, Methodology, Formal analysis, Investigation, Writing – original draft, Read and agreed to the published version of the manuscript. **Jorge Molines:** Methodology, Investigation, Writing – review & editing, Read and agreed to the published version of the manuscript. **M. Esther Gómez-Martín:** Investigation, Writing – review & editing, Funding acquisition, Read and agreed to the published version of the manuscript. **Josep R. Medina:** Investigation, Writing – review & editing, Funding acquisition, Read and agreed to the published version of the manuscript.

## Declaration of competing interest

The authors declare that they have no known competing financial interests or personal relationships that could have appeared to influence the work reported in this paper.

## Notation

*Acronyms*

| | |
|---|---|
| AWACS | Active Wave Absorption System |
| De | Qualitative damage level of destruction defined in Losada et al. (1986) and Vidal et al. (1991) for conventional double-layer armors |
| HeP | Heterogeneous packing defined in Gómez-Martín and Medina (2014). |
| IDa | Qualitative damage level of initiation of damage defined in Losada et al. (1986) and Vidal et al. (1991) for conventional double-layer armors |
| IDe | Qualitative damage level of initiation of destruction defined in Losada et al. (1986) and Vidal et al. (1991) for conventional double-layer armors |
| IIDa | Qualitative damage level of initiation of Irribarren damage defined in Losada et al. (1986) and Vidal et al. (1991) for conventional double-layer armors |
| LASA-V | Local Approximation using Simulated Annealing (Figueres and Medina, 2005) |
| LPC-UPV | Laboratory of Ports and Coasts (UPV) |
| $r$ | Pearson correlation coefficient |
| $R^2$ | Coefficient of determination |
| UPV | Universitat Politècnica de València |

*Symbols*

| | |
|---|---|
| $\Delta = (\rho - \rho_w)/\rho_w$ (−) | Relative submerged mass density of armor units |
| $\xi_m = tan\alpha/(2\pi H_s/[gT_m^2])^{0.5}$ | Surf similarity parameter or Iribarren number calculated using $T_m$ and $H_s$ |
| $\xi_{m0} = tan\alpha/(2\pi H_s/[gT_{m-1,0}^2])^{0.5}$ | Surf similarity parameter obtained with the spectral period $T_{m-1,0}$ |
| $\rho$ (g/cm$^3$) | Mass density of armor unit |
| $\rho_w$ (g/cm$^3$) | Mass density of sea water |
| $\Phi_{0i} = n(1-p_{0i})$ (−) | Initial packing density of the strip $i$ |
| $\Phi_i = n(1-p_i)$ (−) | Packing density of the strip $i$ after the wave attack |
| $a$ (−) | Number of rows in the strip |
| $A_e$ (cm$^2$) | Average eroded cross-section area |
| $cot\alpha$ (−) | Armor slope |
| $C_p = (1 + [D_{n50core}/D_{n50}]^{3/10})^{3/5}$ (−) | Permeability coefficient in Etemad-Shahidi et al. (2020). |
| $d$ (cm) | With of armor band |
| $D\% = N_d/N_T$ | The percentage of displaced units in a reference area |
| $D_n = (W/\rho)^{1/3}$ (cm) | Nominal diameter |
| $D_{n50} = (W_{50}/\rho)^{1/3}$ (cm) | Rock nominal diameter |
| $D_{n50core} = (W_{50}/\rho)^{1/3}$ (cm) | Nominal diameter of rocks in the core |
| $e_i$ | Estimated values |
| $\bar{e}$ | Average of estimated values |
| $g$ (m/s$^2$) | Gravity acceleration |
| $h = h_s(1 + 3m)$ (cm) or (m) | Design water depth defined in Gómez-Martín et al. (2018) |
| $h_s$ (cm) or (m) | Water depth |
| $H$ (cm) or (m) | Characteristic wave height |
| $H_{1/10}$ (cm) or (m) | Average of the one-tenth highest waves |
| $H_{1/3} = H_s$ (cm) or (m) | Average of the one-third highest waves or significant wave height |
| $H_{2\%}$ (cm) or (m) | Wave height exceeded by 2% of the waves |
| $H_{m0} = 4(m_0)^{0.5}$ (cm) or (m) | Spectral significant wave height |
| $I$ (−) | Number of strips |
| $K_D$ (−) | Stability coefficient defined in Hudson (1959) |
| $K_r = H_{m0,r}/H_{m0,i}$ (−) | Reflection coefficient, calculated with the reflected $H_{m0}$, $H_{m0,r}$, and the incident $H_{m0}$, $H_{m0,i}$ |
| $l = bD_n$ (cm) | Band length for Virtual Net method in Gómez-Martín and Medina (2006) |
| $L_m$ (cm) or (m) | Mean wave length close to the model |

| | |
|---|---|
| $L_{0p}$ (cm) or (m) | Local wave length calculated with $T_p$ and $H_{m0}$ |
| $L_p = gT_p^2/(2\pi)$ (cm) or (m) | Deep-water wave length |
| $m$ (%) | Bottom slope |
| $m_i$ (−) | i-th spectral moment |
| $n$ (−) | Number of armor layers |
| $N_d$ (−) | Number of extracted units in a reference area |
| $N_e$ (−) | Number of displaced units from a reference band of the armor of width $d$ |
| $N_i$ (−) | Number of armor units in the strip $i$ |
| $N_{od} = N_e/(d/D_n)$ (−) | Relative damage number defined in Van der Meer (1988b) |
| $N_s = H/\Delta D_n$ | Stability number |
| $N_T$ (−) | Number of units in a reference area |
| $P$ (−) | Structure permeability defined in Van der Meer (1988b) |
| $p_{0i}$ (−) | Initial armor porosity of the strip i |
| $p_i = 1-(N_i D_n^2/(wl))$ (−) | Armor porosity of the strip $i$ after the wave attack |
| $s_m = H_{m0}/L_m$ (−) | Mean wave steepness |
| $s_{0p} = H_{m0}/L_{0p} = 2\pi H_{m0}/(gT_p^2)$ (−) | Peak wave steepness |
| $S = A_e/D_n^2$ (−) | Dimensionless armor damage parameter defined in Broderick (1983) |
| $S_e$ (−) | Equivalent dimensionless armor damage defined in Gómez-Martín and Medina (2006) |
| $T_m$ (s) | Mean temporal wave period |
| $T_{01} = m_0/m_1$ (s) | Mean spectral period |
| $T_{m-1,0} = m_{-1}/m_0$ (s) | Spectral wave period |
| $T_p$ (s) | Wave peak period |
| $w = aDn$ (cm) | Band width for Virtual Net method in Gómez-Martín and Medina (2006) |

## Appendix A. Experimental data in this study

In this section, the experimental data used in this study is summarized. Table 3 shows the equivalent armor damage ($S_e$), the water depth at the toe of the structure ($h_s$), and the spectral wave height ($H_{m0}$) and the peak period ($T_p$) at a distance of $3h_s$ from the toe of the structure estimated with the SwanOne model.

**Table 3**
Summary of the experimental data used in this study.

| Test ID | Armor damage ($S_e$) | $h_s$ (cm) | $H_{m0}$ (cm) | $T_p$ (s) |
|---|---|---|---|---|
| 1 | 0.26 | 20.00 | 7.00 | 1.18 |
| 2 | 0.26 | 20.00 | 8.72 | 1.18 |
| 3 | 0.35 | 20.00 | 9.88 | 1.31 |
| 4 | 0.35 | 20.00 | 10.62 | 1.31 |
| 5 | 0.35 | 20.00 | 11.21 | 1.31 |
| 6 | 0.35 | 20.00 | 11.62 | 1.47 |
| 7 | 0.54 | 20.00 | 12.01 | 1.47 |
| 8 | 0.54 | 20.00 | 12.19 | 1.47 |
| 9 | 0.62 | 20.00 | 12.35 | 1.64 |
| 10 | 0.71 | 20.00 | 12.48 | 1.64 |
| 11 | 0.71 | 20.00 | 12.33 | 1.47 |
| 12 | 0.71 | 20.00 | 12.53 | 1.64 |
| 13 | 0.79 | 20.00 | 12.54 | 1.64 |
| 14 | 0.27 | 20.00 | 8.85 | 1.83 |
| 15 | 0.36 | 20.00 | 10.00 | 1.83 |
| 16 | 0.36 | 20.00 | 10.82 | 2.04 |
| 17 | 0.44 | 20.00 | 11.44 | 2.04 |
| 18 | 0.53 | 20.00 | 11.89 | 2.04 |
| 19 | 0.62 | 20.00 | 12.39 | 2.27 |
| 20 | 0.79 | 20.00 | 12.74 | 2.27 |
| 21 | 0.89 | 20.00 | 12.86 | 2.27 |
| 22 | 0.97 | 20.00 | 13.12 | 2.54 |
| 23 | 1.06 | 20.00 | 13.17 | 2.54 |
| 24 | 1.06 | 20.00 | 13.19 | 2.54 |
| 25 | 0.97 | 20.00 | 13.24 | 2.54 |
| 26 | 0.28 | 30.00 | 7.23 | 1.18 |
| 27 | 0.37 | 30.00 | 8.17 | 1.18 |
| 28 | 0.45 | 30.00 | 9.24 | 1.31 |
| 29 | 0.45 | 30.00 | 10.14 | 1.31 |
| 30 | 0.63 | 30.00 | 11.18 | 1.31 |
| 31 | 0.81 | 30.00 | 12.06 | 1.47 |
| 32 | 0.81 | 30.00 | 12.80 | 1.47 |
| 33 | 0.90 | 30.00 | 13.84 | 1.47 |
| 34 | 1.17 | 30.00 | 14.73 | 1.47 |
| 35 | 1.45 | 30.00 | 15.56 | 1.64 |
| 36 | 1.81 | 30.00 | 16.24 | 1.64 |
| 37 | 2.00 | 30.00 | 16.95 | 1.64 |

**Table 3** (*continued*)

| Test ID | Armor damage ($S_e$) | $h_s$ (cm) | $H_{m0}$ (cm) | $T_p$ (s) |
|---|---|---|---|---|
| 38 | 2.46 | 30.00 | 17.44 | 1.64 |
| 39 | 2.56 | 30.00 | 17.84 | 1.83 |
| 40 | 0.26 | 30.00 | 9.75 | 1.64 |
| 41 | 0.60 | 30.00 | 10.70 | 1.64 |
| 42 | 0.69 | 30.00 | 12.01 | 1.83 |
| 43 | 0.69 | 30.00 | 13.01 | 1.83 |
| 44 | 0.69 | 30.00 | 14.36 | 1.83 |
| 45 | 0.95 | 30.00 | 15.18 | 1.83 |
| 46 | 1.56 | 30.00 | 15.86 | 2.04 |
| 47 | 1.55 | 30.00 | 16.55 | 2.04 |
| 48 | 1.82 | 30.00 | 16.92 | 2.04 |
| 49 | 1.99 | 30.00 | 17.49 | 2.27 |
| 50 | 2.17 | 30.00 | 17.76 | 2.27 |
| 51 | 3.04 | 30.00 | 18.03 | 2.27 |
| 52 | 3.57 | 30.00 | 17.15 | 2.54 |
| 53 | 4.62 | 30.00 | 18.51 | 2.27 |
| 54 | 0.26 | 30.00 | 8.73 | 1.83 |
| 55 | 0.44 | 30.00 | 9.82 | 1.83 |
| 56 | 0.53 | 30.00 | 11.08 | 2.04 |
| 57 | 0.63 | 30.00 | 12.24 | 2.04 |
| 58 | 0.90 | 30.00 | 13.54 | 2.27 |
| 59 | 0.81 | 30.00 | 14.54 | 2.27 |
| 60 | 1.17 | 30.00 | 15.15 | 2.27 |
| 61 | 1.82 | 30.00 | 16.20 | 2.54 |
| 62 | 3.58 | 30.00 | 16.67 | 2.54 |
| 63 | 4.23 | 30.00 | 17.21 | 2.54 |
| 64 | 4.59 | 30.00 | 17.73 | 2.54 |
| 65 | 6.38 | 30.00 | 18.07 | 2.54 |
| 66 | 8.81 | 30.00 | 18.64 | 2.83 |
| 67 | 0.27 | 40.00 | 6.98 | 1.18 |
| 68 | 0.27 | 40.00 | 7.92 | 1.18 |
| 69 | 0.26 | 40.00 | 8.87 | 1.18 |
| 70 | 0.44 | 40.00 | 9.56 | 1.31 |
| 71 | 0.53 | 40.00 | 10.69 | 1.31 |
| 72 | 0.61 | 40.00 | 11.67 | 1.47 |
| 73 | 0.61 | 40.00 | 12.64 | 1.47 |
| 74 | 0.87 | 40.00 | 13.69 | 1.47 |
| 75 | 1.94 | 40.00 | 14.65 | 1.47 |
| 76 | 2.03 | 40.00 | 15.49 | 1.47 |
| 77 | 3.43 | 40.00 | 16.53 | 1.64 |
| 78 | 5.29 | 40.00 | 17.55 | 1.64 |
| 79 | 7.65 | 40.00 | 18.37 | 1.64 |
| 80 | 9.57 | 40.00 | 19.04 | 1.64 |

## References

Argente, G., 2019. Estudio de la estabilidad hidráulica de diques en talud rebasables protegidos con mantos de escollera, cubos y Cubípodos. PhD Thesis (in Spanish). Universitat Politècnica de València, Valencia (Spain). https://doi.org/10.4995/Thesis/10251/134362.

Battjes, J.A., Groenendijk, H.W., 2000. Wave height distributions on shallow foreshores. Coast. Eng. 40, 161–182. https://doi.org/10.1016/S0378-3839(00)00007-7.

Broderick, L.L., 1983. Riprap stability a progress report. In: Proc. Specialty Conference on Design, Construction, Maintenance and Performance of Coastal Structures. ASCE, Arlingtion, VA, pp. 320–330.

Díaz-Carrasco, P., Moragues, M.V., Clavero, M., Losada, M.A., 2020. 2D water-wave interaction with permeable and impermeable slopes: dimensional analysis and experimental overview. Coast. Eng. 158, 103682 https://doi.org/10.1016/j.coastaleng.2020.103682.

Etemad-Shahidi, A., Bali, M., Van Gent, M.R.A., 2020. On the stability of rock armored rubble mound structures. Coast. Eng. 158, 103655 https://doi.org/10.1016/j.coastaleng.2020.103655.

Figueres, M., Medina, J.R., 2005. Estimating incident and reflected waves using a fully nonlinear wave model. In: Proc. 29th International Conference on Coastal Engineering. Lisboa (Portugal), pp. 594–603. https://doi.org/10.1142/9789812701916-0047.

Gómez-Martín, M.E., Medina, J.R., 2006. Damage progression on cube armored breakwaters. In: Proc. 30th International Conference on Coastal Engineering. World Scientific Publishing Company, pp. 5229–5240. https://doi.org/10.1142/9789812709554_0438.

Gómez-Martín, M.E., Medina, J.R., 2014. Heterogeneous packing and hydraulic stability of cube and Cubipod armor units. J. Waterw. Port, Coast. Ocean Eng. 140, 100–108. https://doi.org/10.1061/(ASCE)WW.1943-5460.0000223.

Gómez-Martín, M.E., 2015. Análisis de la evolución de averías en el manto principal de diques en talud formado por escolleras, cubos y Cubípodos. PhD Thesis (in Spanish). Universitat Politècnica de València, Valencia (Spain). https://doi.org/10.4995/Thesis/10251/59231.

Gómez-Martín, M.E., Herrera, M.P., Gonzalez-Escriva, J., Medina, J.R., 2018. Cubipod® armor design in depth-limited regular wave-breaking conditions. J. Mar. Sci. Eng. 6, 150. https://doi.org/10.3390/jmse6040150.

Herrera, M.P., Gómez-Martín, M.E., Medina, J.R., 2017. Hydraulic stability of rock armors in breaking wave conditions. Coast. Eng. 127, 55–67. https://doi.org/10.1016/j.coastaleng.2017.06.010.

Hudson, R.Y., 1959. Laboratory investigation of rubble-mound breakwaters. J. Waterw. Harb. Div. 85, 93–121. https://doi.org/10.1061/JWHEAU.0000142.

Losada, M.A., Desire, J.M., Alejo, L.M., 1986. Stability of blocks as breakwater armor units. J. Struct. Eng. 112, 2392–2401. https://doi.org/10.1061/(ASCE)0733-9445(1986)112:11(2392).

Mares-Nasarre, P., Argente, G., Gómez-Martín, M.E., Medina, J.R., 2019. Overtopping layer thickness and overtopping flow velocity on mound breakwaters. Coast. Eng. 154, 103561 https://doi.org/10.1016/J.COASTALENG.2019.103561.

Mares-Nasarre, P., Argente, G., Gómez-Martín, M.E., Medina, J.R., 2020a. Influence of mild bottom slopes on the overtopping flow over mound breakwaters under depth-limited breaking wave conditions. J. Mar. Sci. Eng. 8 https://doi.org/10.3390/JMSE8010003.

Mares-Nasarre, P., Molines, J., Gómez-Martín, M.E., Medina, J.R., 2020b. Individual wave overtopping volumes on mound breakwaters in breaking wave conditions and gentle sea bottoms. Coast. Eng. 159, 103703 https://doi.org/10.1016/j.coastaleng.2020.103703.

Mares-Nasarre, P., Argente, G., Gómez-Martín, M.E., Medina, J.R., 2021a. Armor damage of overtopped mound breakwaters in depth-limited breaking wave conditions. J. Mar. Sci. Eng. 9, 952. https://doi.org/10.3390/jmse9090952.

Mares-Nasarre, P., Molines, J., Gómez-Martín, M.E., Medina, J.R., 2021b. Explicit Neural Network-derived formula for overtopping flow on mound breakwaters in depth-limited breaking wave conditions. Coast. Eng. 164, 103810 https://doi.org/10.1016/j.coastaleng.2020.103810.

Medina, J.R., Molines, J., Gómez-Martín, M.E., 2014. Influence of armour porosity on the hydraulic stability of cube armour layers. Ocean Eng. 88, 289–297. https://doi.org/10.1016/j.oceaneng.2014.06.012.

MFOM, 2012. Diques de abrigo en los puertos de Interes General del Estado. Años 1986-2011, 2012. Ministerio de Fomento – Puertos del Estado, Madrid, p. 346 (in Spanish).

Molines, J., Medina, J.R., 2016. Explicit wave-overtopping formula for mound breakwaters with crown walls using CLASH neural network–derived data. J. Waterw. Port, Coast. Ocean Eng. 142 (3) https://doi.org/10.1061/(ASCE)WW.1943-5460.0000322, 04015024-1-04015024-13.

MOPU, 1988. Diques de Abrigo en España. Tomo 1 – Fachadas Norte y Galicia, 1988. Ministerio de Obras Públicas y Urbanismo – Dirección General de Puertos y Costas, Madrid, p. 548 (in Spanish).

Smith, G., Wallast, I., Van Gent, M.R.A., 2003. Rock slope stability with shallow foreshores. In: Proc. 28th International Conference on Coastal Engineering. World Scientific Publishing Company, pp. 1524–1536. https://doi.org/10.1142/9789812791306_0128.

Thompson, D.M., Shuttler, R.M., 1975. Riprap Design for Wind Wave Attack. A Laboratory Study in Random Waves. Report EX 707, Hydraulic Research, Wallingford.

USACE, 1975. Shore Protection Manual, U.S. Army Coastal Engineering Research Center U.S. Army Engineer Waterways Experiment Station. Vicksburg, Mississippi.

USACE, 1984. Shore Protection Manual, U.S. Army Coastal Engineering Research Center. U.S. Army Engineer Waterways Experiment Station, Vicksburg, Mississippi.

Van der Kreek, J., 1969. J. Waterw. Harb. Div. 95.3, 345–354.

Van der Meer, J.W., 1988a. Rock Slopes and Gravel Beaches under Wave Attack. PhD Thesis. Technical University of Delft.

Van der Meer, J.W., 1988b. Stability of cubes, tetrapods and accropode. In: Design of Breakwaters. Thomas Telford Publishing, pp. 71–80. https://doi.org/10.1680/dob.13513.0007.

Van der Meer, J.W., 1999. Design of Concrete Armour Layers. Proc. Coastal Structures '99, 1. A.A.Balkema, Rotterdam, pp. 213–221, 2000.

Van Gent, M.R.A., Smale, A.J., Kuiper, C., 2004. Stability of rock slopes with shallow foreshores. In: Proc. Coastal Structures 2003. American Society of Civil Engineers, Reston, VA, pp. 100–112. https://doi.org/10.1061/40733(147)9.

Verhagen, H.J., van Vledder, G., Arab, S.E., 2008. A practical method for design of coastal structures in shallow water. In: Proc. 31st International Conference on Coastal Engineering. World Scientific Publishing Company, pp. 2912–2922. https://doi.org/10.1142/9789814277426_0241.

Vidal, C., Losada, M.A., Medina, R., 1991. Stability of mound breakwater's head and trunk. J. Waterw. Port, Coast. Ocean Eng. 117, 570–587. https://doi.org/10.1061/(ASCE)0733-950X(1991)117:6(570).

Vidal, C., Medina, R., Lomónaco, P., 2006. Wave height parameter for damage description of rubble-mound breakwaters. Coast. Eng. 53, 711–722. https://doi.org/10.1016/j.coastaleng.2006.02.007.